Transition Met Chem (2011) 36:489–498
DOI 10.1007/s11243-011-9494-y

DNA-binding, antioxidant activity and solid-state fluorescence studies of copper(II), zinc(II) and nickel(II) complexes with a Schiff base derived from 2-oxo-quinoline-3-carbaldehyde

Zeng-Chen Liu · Zheng-Yin Yang · Tian-Rong Li · Bao-Dui Wang · Yong Li · Ming-Fang Wang

Received: 19 January 2011 / Accepted: 18 April 2011 / Published online: 6 May 2011

Abstract A Schiff base derived from 2-oxo-quinoline-3-carbaldehyde-4-aminophenazone and its Cu(II), Zn(II) and Ni(II) complexes were synthesized. The molecular structures of the Zn(II) and Ni(II) complexes were determined by X-ray crystal diffraction. The DNA-binding modes of the compounds were investigated by spectroscopic methods, viscosity measurements and ethidium bromide-DNA displacement experiments. The experimental evidence indicated the compounds interact with calf thymus DNA through intercalation. Additionally, the compounds exhibited potential antioxidant properties in in vitro studies, and the Cu(II) complex was the most effective. The solid-state fluorescence properties of the Zn(II) complex were studied.

Introduction

Ever since the discovery of *cis*-platin as an anticancer agent, investigation into the interactions of transition metal complexes with DNA has been pursued, because of their utility as DNA footprinting agents, structural probes, sequence-specific cleavage agents and potential antitumor drugs [1–4]. We have focused on the DNA-binding properties of metal complexes derived from biologically active small molecules such as quinoline, flavone and coumarin [5, 6]. The non-covalent interactive modes, which include intercalation, groove binding and electrostatic binding, are important in the biological activity of many drugs and the mechanisms by which DNA replication is inhibited in cancer cells. Biological activities such as antitumor, antimalarial and antibacterial activities are all relevant to the binding modes of DNA to drugs [7, 8]. Hence, studies on interactive modes of transition metal complexes with DNA can provide us with new insights, not only for the design of drugs but also to develop highly sensitive diagnostic agents.

Quinoline derivatives have attracted much attention during the last decades due to their potential application as antibacterial drugs that effectively inhibit DNA replication [9, 10]. It has been reported that some transition metal complexes with quinoline derivatives exhibit excellent DNA-binding and biological activities [11, 12]. Many Schiff base complexes have been investigated extensively owing to the good coordination properties of such ligands and attractive biological activities of the complexes [13–19]. In this paper, the synthesis, characterization and DNA-binding activities of new transition metal complexes (Cu, Zn, Ni) with quinoline-2-one-3-carbaldehyde-4-aminophenazone Schiff base are presented. The structures of the Zn(II) and Ni(II) complexes have been characterized by X-ray crystallography. The DNA-binding activities have been investigated by UV–Vis spectroscopic titration, fluorescence spectra and viscosity measurements. Furthermore, the intrinsic binding constants have been determined by fluorescence titration. As reported in previous papers, some transition metal complexes exhibit potential antioxidant activities [20–23]. Since free radicals such as hydroxyl are relevant to many diseases such as Alzheimers and Parkinsons [24], the investigation into hydroxyl radical scavenging by metal complexes is of interest.

Z.-C. Liu · Z.-Y. Yang (✉) · T.-R. Li · B.-D. Wang · Y. Li · M.-F. Wang
College of Chemistry and Chemical Engineering and State Key Laboratory of Applied Organic Chemistry, Lanzhou University, 730000 Lanzhou, People's Republic of China
e-mail: yangzy@lzu.edu.cn

Z.-C. Liu · Z.-Y. Yang · T.-R. Li · B.-D. Wang · Y. Li · M.-F. Wang
Key Laboratory of Nonferrous Metal Chemistry and Resources Utilization of Gansu Province, Lanzhou University, 730000 Lanzhou, People's Republic of China

The Zn(II) complex, which emits Kelly fluorescence under UV light, exhibits excellent solid-state luminescence properties, as reported in this paper.

Experimental

Calf thymus DNA (CT-DNA) and EB (Ethidium bromide) were purchased from Sigma. The CT-DNA was dissolved in double distilled deionized water. The concentrations of DNA were determined using the molar extinction coefficient of 6,600 M^{-1} cm^{-1}. Acetanilide was purchased from Guang Fu Chemical Co, Tianjin, China. All materials and solvents were of analytical reagent grade quality and were used without further purification. All spectroscopic measurements were taken in Tris–HCl buffer (pH = 7.2) containing 5 mM tris [Tris (hydroxymethyl)-amino methane] and 50 mM NaCl.

^{1}H-NMR spectra were recorded on a Varian VR300-MHz spectrometer with TMS as an internal standard. Melting points were determined on a Beijing XT4-100X microscopic melting point apparatus. ESI-MS spectra were recorded on an Esquire 6000 mass spectrograph. UV–Vis spectra were recorded on a Perkin-Elmer Lambda-35 UV–Vis spectrophotometer. Fluorescence spectra were obtained on a Shimadzu RF-5301 spectrophotometer at room temperature. Molar conductivity measurements were taken with a DDS-11C type conductivity bridge using 1.0×10^{-3} mol/L solutions in ethanol at 25 °C. IR spectra were recorded on a Thermo Mattson FTIR instrument using KBr discs in the 4,000–400 cm^{-1} region.

Synthesis of the ligand

As shown in Scheme 1, 2-oxo-quinoline-3-carbaldehyde was prepared according to the literature [25, 26]. An ethanol solution (10 mL) of 4-aminophenazone (0.71 g, 3.5 mmol) was added to an ethanol solution (10 mL) of 2-oxo-quinoline-3-carbaldehyde (0.6 g, 3.5 mmol). The mixture was stirred under reflux for 12 h, where upon a white precipitate separated out. The precipitate was filtrated off and washed with ethanol. Recrystallization from DMF/H_2O (V:V = 1:1) gave the ligand HL, which was dried under vacuum. Yield, 1.16 g, 85%. m.p: 307–309 °C. ^{1}H–NMR (DMSO-d_6 400 MHz): δ 11.95 (1H, s, –N^1–H), δ 9.75 (1H, s, –CH=N), δ 8.54 (1H, s, –C^4–H), δ 7.83–7.81 (1H, J = 8, d, –C^8–H), δ 7.55–7.50 (3H, overlap, –$C^{10',14',12'}$–H), δ 7.39–7.36 (3H, overlap, –$C^{11',13',6}$–H), δ 7.33–7.31 (1H, J = 8, d, –C^5–H), δ 7.22–7.18 (1H, J = 16, m, –C^7–H), δ 3.30 (3H, s, –$C^{7'}$–H), δ 3.20 (3H, s, –$C^{5'}$–H). IR (KBr) cm^{-1}: ν (C=O)$_{2\text{-oxo-quinoline}}$ 1,654, ν (C=O)$_{4\text{-aminophenazone}}$ 1,652, ν (C=N) 1,622.

Preparation of the complexes

HL (0.2 mmol, 0.0716 g) and Cu(II) nitrate (0.2 mmol, 0.0483 g) were added to ethanol (10 mL). After stirring for 5 min, the mixture was filtered to remove insoluble residues and then stirred under reflux for 10 h. The resulting green precipitate (yield: 0.096 g, 85%) of the Cu(II) complex was filtered off, washed several times with ethanol and dried for 24 h under vacuum. Anal. Calcd for $C_{21}H_{20}N_6O_9Cu$ (%): C, 44.7; H, 3.6; N, 14.9. Found (%): C, 45.7; H, 3.6; N, 14.5. ESI-MS (CH_3OH, m/z): 439.2, IR (KBr) cm^{-1}: ν (C=O)$_{2\text{-oxo-quinoline}}$ 1,642, ν (C=O)$_{4\text{-aminophenazone}}$ 1,639, ν (C=N) 1,615, ν (NO_3^-) 1,384.

The Zn(II) and Ni(II) complexes were prepared by the same method as for the Cu(II) complex. Zn(II) complex: Yield, 80%, Colour yellow, Anal. Calcd for $C_{21}H_{24}N_5O_{11}Zn$ (%): C, 41.9; H, 4.0; N, 13.9. Found (%): C, 41.7; H, 4.0; N, 13.5. IR (KBr) cm^{-1}: ν (C=O)$_{2\text{-oxo-quinoline}}$ 1,642, ν (C=O)$_{4\text{-aminophenazone}}$ 1,638, ν (C=N) 1,614, ν (NO_3^-) 1,383. Ni(II) complex: Yield, 75%, Colour green. Anal. Calcd for $C_{21}H_{24}N_5O_{11}Ni$ (%): C, 42.4; H, 4.1; N, 14.1. Found (%): C, 42.6; H, 3.9; N, 14.1. IR (KBr) cm^{-1}: ν (C=O)$_{2\text{-oxo-quinoline}}$ 1,644, ν (C=O)$_{4\text{-aminophenazone}}$ 1,639, ν (C=N) 1,615, ν (NO_3^-) 1,384.

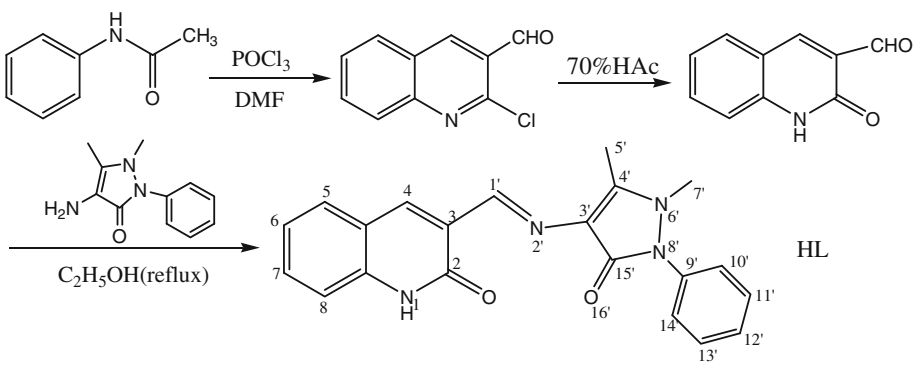

Scheme 1 Synthesis of ligand (2-oxo-quinoline-3-carbaldehyde-4-aminophenazone Schiff base)

X-ray crystallography

A yellow crystal of the Zn(II) complex was mounted on a Bruker Smart-1000 CCD diffractometer with graphite-monochromated Mo-kα radiation ($\lambda = 0.71073$Å) at 296(2) K. The intensity data were collected by the ω scan mode within $2.32 < \theta < 28.49°$ for hkl ($-11 \leq h \leq 12$, $-14 \leq k \leq 13$, $-17 \leq l \leq 17$) in the Triclinic crystal system. The positions and anisotropic thermal parameters of all non-hydrogen atoms were refined on F^2 by full-matrix least-squares techniques with the SHELX-97 program package (G. M. Sheldrick, Bruker AXS, Madison, WI, 2001). Absorption corrections were employed using semi-empirical methods from equivalents.

A green crystal of the Ni(II) complex was measured on a Bruker Smart-1000 CCD diffractometer with graphite-monochromated Mo-kα radiation ($\lambda = 0.71073$Å) at 296(2) K. The intensity data were collected by the ω scan mode within $2.31 < \theta < 28.40°$ for hkl ($-11 \leq h \leq 11$, $-14 \leq k \leq 14$, $-17 \leq l \leq 17$) in the Triclinic crystal system. The positions and anisotropic thermal parameters of all non-hydrogen atoms were refined on F^2 by full-matrix least-squares techniques with the SHELX-97 program package. Absorption corrections were employed using semi-empirical methods from equivalents.

DNA-binding study methods

UV–Vis absorption titration experiments were performed by maintaining a constant concentration of the compounds (10 μM) and gradually increasing the concentration of CT-DNA. The compounds were dissolved in a mixed solvent of 1% methanol and 99% Tris–HCl buffer. The reference solution was the corresponding Tris–HCl buffer solution. When measuring the absorption spectra, equal amounts of CT-DNA were added to both the compound and reference solutions to eliminate the absorbance of CT-DNA itself. The sample solution was scanned in the range 200–500 nm.

For the fluorescence spectroscopic titrations, fixed amounts of the compounds (10 μM) were titrated with increasing amounts of CT-DNA. The samples were excited at 375 nm, and the fluorescence emission intensity was monitored at 501 nm. K values were determined using the following equation [27];

$$r/C_f = K(1 - nr)$$

where $r = C_b/[DNA]$, $C_f = C_t$ $[(F-F_0)/(F_{max}-F_0)]$, and C_b and C_t are the concentrations of free compound and total compound, respectively. F is the observed fluorescence emission intensity at a given DNA concentration, F_0 is the intensity in the absence of DNA and F_{max} is the fluorescence intensity of the totally bound compound. Binding data were analysed using a Scatchard plot of (r/C_f) versus r. All experiments were conducted at 20 °C in a buffer containing 5 mM Tris–HCl (pH = 7.2) and 50 mM NaCl.

The viscosity measurements were obtained using an Ubbelohde viscometer in a water bath maintained at 298.0 (±0.1) K. The DNA concentration was kept constant (5 μM), and the concentration of test compound was gradually increased (0.5–3.5 μM). The solution's flow time through the capillary was determined to the nearest 0.02 s using a stopwatch. Each sample was measured three times, and then an average flow was calculated. Data were analysed as $(\eta/\eta_0)^{1/3}$ versus the ratio of the concentration of the compound to CT-DNA, where η is the viscosity of CT-DNA in the presence of the compound, and η_0 is the viscosity of CT-DNA alone. Viscosities were calculated from the observed flow times of solutions containing CT-DNA corrected for the flow time of buffer alone (t_0), $\eta = t - t_0$.

Ethidium bromide experiments were conducted by adding solutions of the compounds to the Tris–HCl buffer containing EB-DNA. The change in fluorescence intensity was recorded using excitation and emission wavelengths of 521 and 587 nm, respectively.

Hydroxyl radical scavenger measurements

Hydroxyl radicals in aqueous media were generated using the Fenton system [28, 29]. Solutions of the test complexes were prepared with double distilled water. The 5 mL assay mixture contained the following reagents: safranin (11.4 μM), EDTA-Fe(II) (40 μM), H_2O_2 (1.76 mM), the test complex (1–6 μM) and a phosphate buffer (67 μM, pH = 7.4). The assay mixtures were incubated at 30 °C for 10 min in a water bath. The absorbance was then measured at 520 nm. All the tests were run in triplicate and are expressed as the mean and standard deviation (SD) [30]. The scavenging ratio is defined as

$$\text{Scavenging ratio}\,(\%) = [(A_i - A_0)/(A_c - A_0)] \times 100$$

where A_i = absorbance in the presence of the test compound; A_0 = absorbance of the blank in the absence of the test compound; A_c = absorbance in the absence of the tested compound, EDTA-Fe(II) and H_2O_2.

Solid-state fluorescence experiments were performed at room temperature with a slit width of 1.5 nm for both entrance and exit slits. The excitation wavelength was 393 nm, and the emission wavelength was 513 nm for all compounds.

Results and discussion

Characterization and structures of the complexes

The free ligand and its two complexes are soluble in ethanol, methanol, DMF and DMSO, but insoluble in water or

diethyl ether. They are all air stable. Crystals of the Zn(II) and Ni(II) complexes were obtained by evaporating methanol solutions. The formulation of the Cu(II) complex was established by its molar conductivity, elemental analyses, ESI-MS spectra and IR data.

The molar conductivity of the Cu(II) complex in methanol is 196 S m^2 mol^{-1}, which is in the range expected for a 1:2 electrolyte. The elemental analysis suggests the empirical formula $Cu^{\cdot}HL^{\cdot}(NO_3)_2^{\cdot}H_2O$, and this is supported by the electrospray ionization (ESI) mass spectrum (*m/z*: 439.2), which can be assigned to the ion $[Cu^{\cdot}HL^{\cdot}H_2O]^+$ $(M–2NO_3^-)$.

The IR spectra of the free ligand and Cu(II) complex were compared. The IR spectrum of the free ligand shows bands at 1,654 and 1,652 cm^{-1}, which are attributed to the stretching vibrations ν $(C=O)_{2\text{-oxo-quinoline}}$ and ν $(C=O)_{4\text{-aminophenazone}}$, respectively. These have been replaced by bands at 1,642 and 1,639 cm^{-1} in the spectrum of the Cu(II) complex. A band at 1,604 cm^{-1} for the free ligand is assigned to the ν (C=N) stretch, which shifts to 1,595 cm^{-1} upon coordination of the nitrogen atom to copper. Additionally, an intense band associated with the asymmetric stretching of nitrate is observed at 1,384 cm^{-1}, establishing that the Cu(II) complex contains free nitrate (C_{2v}). All these results suggest that the formula of the Cu(II) complex is $[Cu^{\cdot}HL^{\cdot}H_2O]^{\cdot}(NO_3)_2$. The IR spectra of the Ni(II) and Zn(II) complexes are consistent with that of the Cu(II) complex.

Crystal structures of the Zn(II) and Ni(II) complexes

The crystallographic data for the Zn(II) complex are given in Table 1. An ORTEP representation of the complex, including the atom numbering scheme, is shown in Fig. 1, and selected bond lengths and angles are listed in Table 2. The complex is mononuclear, and the coordination of the ligand to Zn(II) results in the formation of both five-membered (ZnOCCN) and six-membered (ZnNCCCO) chelate rings. The coordination configuration of Zn(II) with $N^3O^1O^2O^4O^6O^7$ shows a classic six-membered ring. There are also one water molecule and nitrate, which do not take part in coordination, within the crystal lattice. The asymmetric unit cell consists of two crystallographically independent molecules of the Zn(II) complex.

The crystallographic data for the Ni(II) complex are given in Table 1. An ORTEP representation of the structure, including the atom numbering scheme, is shown in Fig. 2 and selected bond lengths and angles are listed in Table 3. Compared with the Zn(II) complex, the coordination of the Ni(II) complex shows very similar chelating rings (octahedral geometry). There are also one non-coordinated water molecule and one nitrate in the crystal lattice. The asymmetric unit cell contains two crystallographically independent molecules of the Ni(II) complex.

Table 1 Crystal data and structure refinement of Zn(II) and Ni(II) complexes

	ZnL	NiL
Formula	$C_{21}H_{24}N_6O_{11}Zn$	$C_{21}H_{24}N_6O_{11}Ni$
FW	601.85	595.15
Crystal colour	Yellow	Green
Crystal size(mm)	0.35 × 0.32 × 0.29	0.34 × 0.31 × 0.29
Crystal system	Triclinic	Triclinic
Space group	P-1	P-1
a (Å)	9.011 (6)	8.9514 (17)
b (Å)	10.926 (8)	10.924 (2)
c (Å)	13.289 (9)	13.163 (2)
α (°)	80.948 (9)	81.253 (2)
β (°)	78.757 (8)	78.334 (2)
γ (°)	82.467 (8)	82.422 (2)
V (Å^3)	1,260.4 (15)	1,239.0 (4)
Z	2	2
D_{calc} (g/cm^3)	1.586	1.595
Abs coeff (mm^{-1})	1.046	0.856
F (000)	620.0	616
$\theta_{min\ and\ max(deg)}$	2.32–28.49	2.31–28.40
Reflections collected	3,249/6,379	4,578/6,221
Unique	[*R*(int) = 0.0510]	[*R*(int) = 0.0235]
Final *R* indices	*R*1 = 0.0651	*R*1 = 0.0387
[I >2 sigma(I)]	w*R*2 = 0.1503	w*R*2 = 0.0922
R indices (all data)	*R*1 = 0.1201,	*R*1 = 0.0545,
	w*R*2 = 0.1790	w*R*2 = 0.1004

DNA-binding mode and affinity

The binding modes of compounds to CT-DNA are classically characterized through electronic absorption titrations. When the compounds intercalate with the base pairs of DNA, the π^* orbitals of the intercalated compounds can couple with the π orbitals of the base pairs, thus decreasing the π–π^* transition energies. On the other hand, the coupling π^* orbitals are partially filled by electrons, thus decreasing the transition probabilities [31]. Therefore, intercalative interaction can result in both hypochromism and red shift, as reported previously [32]. As shown in Fig. 3, the absorption bands of the free ligand and its Cu, Zn and Ni complexes at 380 nm exhibit hypochromism of about 50.0, 75.0, 76.5 and 77.8%, respectively, which are characteristic of intercalation in the presence of CT-DNA [33]. Hence, high-affinity interactions between CT-DNA and these compounds are indicated; however, the binding mode needs to be confirmed by more experiments.

Fluorescence emission spectroscopy can provide diagnostic evidence to distinguish the binding modes of different compounds to DNA [34]. The present compounds emit weak luminescence in Tris–HCl buffer with a

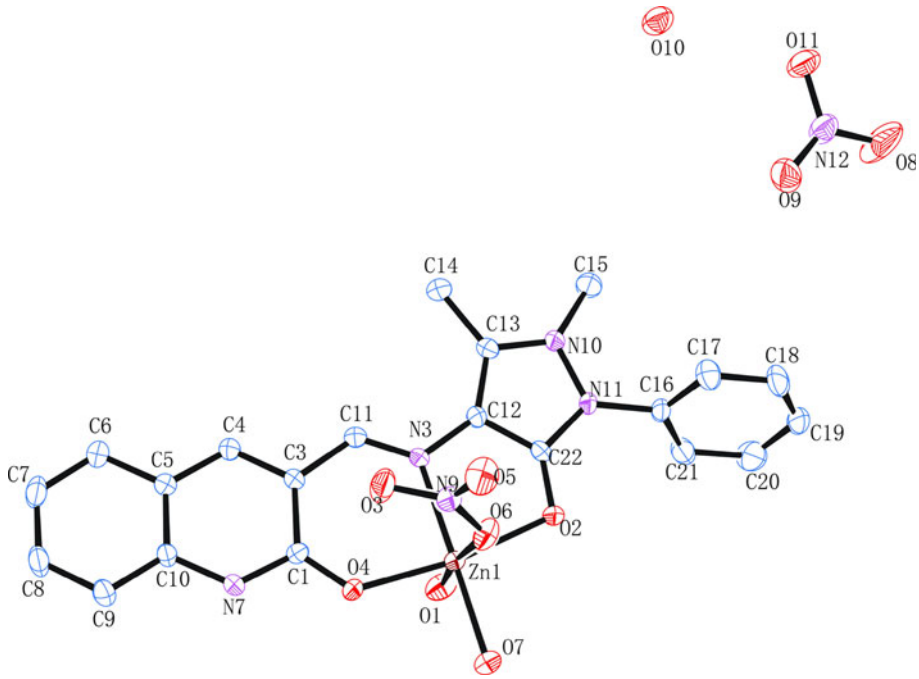

Fig. 1 ORTEP view of [ZnL] showing the atom numbering of scheme and 50% thermal ellipsoids probability for the non-hydrogen atoms

Table 2 Selected bond lengths (Å) and angles (°) for ZnL

Bond names	Bond lengths	Bond angles	Angle
Zn1–O4	2.035(3)	O4–Zn1–O7	89.97(16)
Zn1–N3	2.118(4)	O4–Zn1–N3	88.88(13)
Zn1–O7	2.057(4)	O7–Zn1–N3	177.09(16)
Zn1–O1	2.120(4)	O4–Zn1–O1	90.57(16)
Zn1–O2	2.157(3)	O7–Zn1–O1	92.13(18)
Zn1–O6	2.178(3)	N3–Zn1–O1	90.55(16)
O2–C22	1.274(5)	O4–Zn1–O2	170.93(11)
N3–C11	1.276(5)	O7–Zn1–O2	99.09(15)
N3–C12	1.396(6)	N3–Zn1–O2	82.10(13)
O4–C1	1.253(5)	O1–Zn1–O2	88.55(16)
C16–N11	1.437(5)	O4–Zn1–O6	96.57(14)
N7–C1	1.355(6)	O7–Zn1–O6	85.52(16)
N7–C10	1.387(5)	N3–Zn1–O6	91.96(14)
N10–C13	1.336(6)	O1–Zn1–O6	172.48(15)
N10–C11	1.393(5)	O2–Zn1–O6	84.78(13)
N10–C15	1.458(6)	C22–O2–Zn1	106.0(3)
N11–C22	1.358(5)	C11–N3–C12	125.0(4)
C19–C20	1.354(9)	C11–N3–Zn1	126.3(3)
O9–N12	1.211(6)	C12–N3–Zn1	108.5(3)
N12-O8	1.196(6)	C1–O4–Zn1	128.5(3)
N12–O11	1.268(5)	C17–C16–N11	120.4(4)
O6–N9	1.273(5)	C1–N7–C10	126.5(4)
O5–N9	1.232(5)	C13–N10–N11	109.5(4)
N9–O3	1.231(5)	C13–N10-C15	128.5(4)

maximum at 450 nm. The fluorescence titration spectra of the compounds with DNA were obtained at constant concentrations of the test compounds. Figure 4 displays the

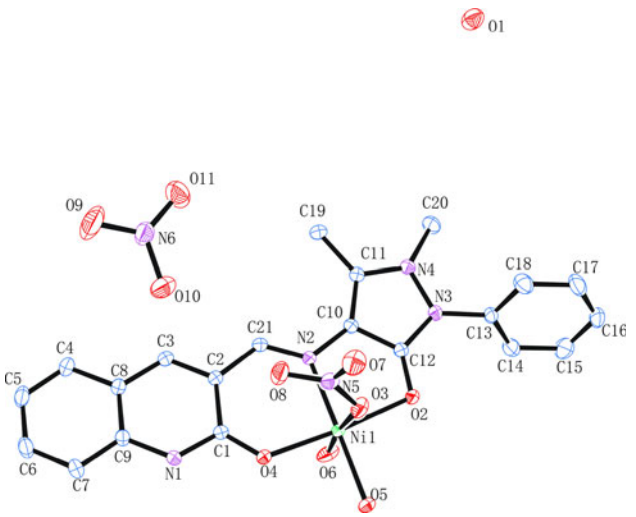

Fig. 2 ORTEP view of [NiL] showing the atom numbering of scheme and 50% thermal ellipsoids probability for the non-hydrogen atoms

resulting titration curves. The fluorescence intensity of these compounds was enhanced dramatically with the addition of CT-DNA, which clearly indicates that all of the compounds can insert into the hydrophobic environment inside the DNA helix. This results in the protection from the solvent water molecules, leading to enhancement of the fluorescence intensity [35]. Enhanced fluorescence is believed to be one of the criteria for intercalative binding [36, 37]. According to the Scatchard equation, a plot of r/C_f versus r gives the intrinsic binding constants of the compounds. Thus, CuL ($K = 8.74 \times 10^5$ M^{-1}) interacts with

Table 3 Selected bond lengths (Å) and angles (°) for NiL

Bond names	Bond lengths	Bond angles	Angle
Ni1–O4	2.0044(15)	O4–Ni1–N2	91.18(6)
Ni1–N2	2.0348(16)	O4–Ni1–O5	88.19(7)
Ni1–O5	2.0447(17)	N2–Ni1–O5	179.37(7)
Ni1–O6	2.0658(18)	O4–Ni1–O6	89.68(8)
Ni1–O3	2.0890(16)	N2–Ni1–O6	90.34(7)
Ni1–O2	2.1272(14)	O5–Ni1–O6	89.64(8)
N2–C21	1.291(2)	O4–Ni1–O3	96.19(7)
N2–C10	1.392(3)	N2–Ni1–O3	93.25(7)
O2–C12	1.265(2)	O5–Ni1–O3	86.83(7)
O4–C1	1.247(2)	O6–Ni1–O3	173.05(7)
O3–N5	1.268(2)	O4–Ni1–O2	174.96(5)
N3–C12	1.364(3)	N2–Ni1–O2	83.88(6)
N1–C1	1.352(3)	O5–Ni1–O2	96.75(6)
N1–C9	1.387(3)	O6–Ni1–O2	89.34(7)
N5–O8	1.227(2)	O3–Ni1–O2	85.14(6)
N5–O7	1.242(2)	C21–N2–C10	124.32(17)
N3–N4	1.390(2)	C21–N2–Ni1	126.51(14)
N4–C11	1.341(3)	C10–N2–Ni1	109.04(12)
N4–C20	1.460(3)	C12–O2–Ni1	104.55(12)
O10–N6	1.250(3)	C1–O4–Ni1	127.28(14)
O9–N6	1.207(3)	N5–O3–Ni1	127.98(13)
C9–C8	1.393(3)	O2–C12–N3	126.50(18)
N6–O11	1.218(3)	O4–C1–N1	117.75(18)
C5–C6	1.397(4)	O4–C1–C2	126.42(19)

DNA more strongly than the free ligand ($K = 5.34 \times 10^5\ M^{-1}$), and also the ZnL ($K = 6.21 \times 10^5\ M^{-1}$) and NiL ($K = 7.15 \times 10^5\ M^{-1}$) complexes. We further characterized the binding to DNA by viscosity studies and ethidium bromide (EB) competitive experiments.

Measurements of DNA viscosity, which is sensitive to DNA length change, are regarded as the least ambiguous and the most critical test of binding in solution in the absence of crystallographic structural data [38, 39]. In classic intercalation, the DNA helix lengths are separated to accommodate the ligand, leading to an increase in DNA viscosity. In contrast, groove binding and electrostatic modes result in unchanged length of DNA helix and no alteration in DNA viscosity. Figure 5 shows that the present compounds cause a significant increase in the viscosity of CT-DNA, which follows the order CuL > NiL > ZnL > L. The results suggest classical intercalation of the planar ligand. As with the fluorescence experiments, the Cu(II) complex exhibits higher affinity with CT-DNA than the other compounds.

Ethidium bromide is one of the most sensitive fluorescent probes which can bind to DNA through intercalation [40, 41]. Competitive binding with EB can provide rich information with regard to the DNA-binding mode. As shown in Fig. 6, the fluorescence intensity of ethidium bromide decreases obviously upon addition of the test compounds. The K_q values for the compounds are $0.71 \times 10^5\ M^{-1}$ (L), $2.34 \times 10^5\ M^{-1}$ (CuL), $K_q = 1.03$

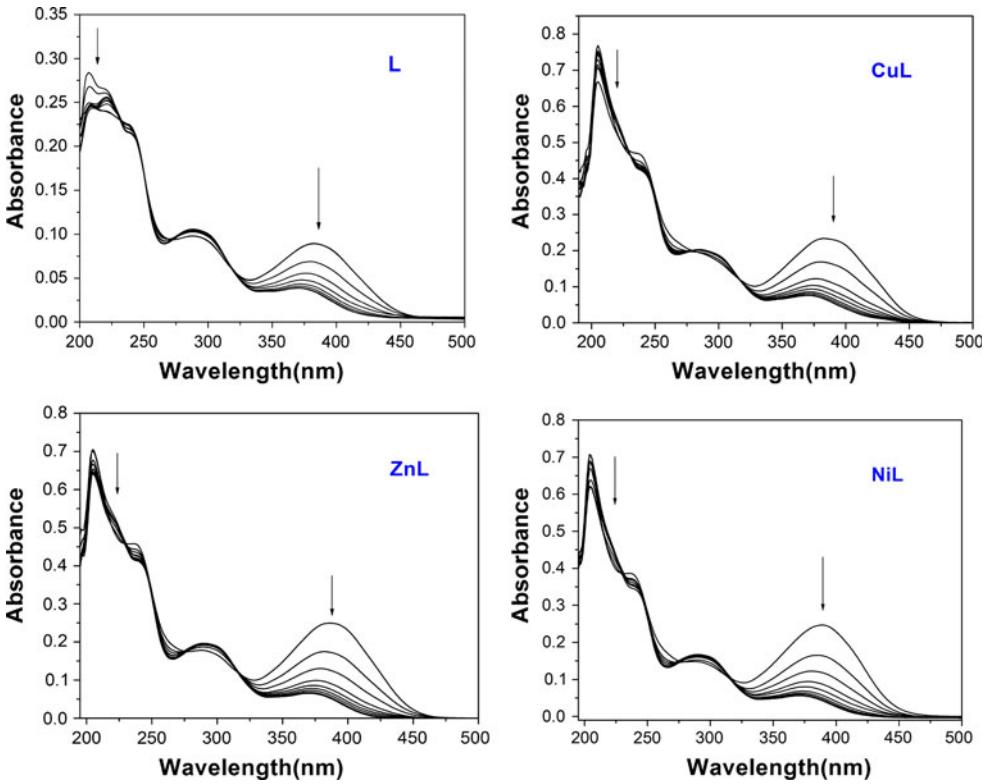

Fig. 3 Absorption spectra of compounds (10 μM) in the absence and presence of increasing amounts of CT-DNA (2.5, 5, 7.5, 10, 12.5, 15, 17.5, 20, 22.5, 25, 27.5, 30 μM; subsequent spectra). The *arrow* shows the absorbance changes upon increasing DNA concentration

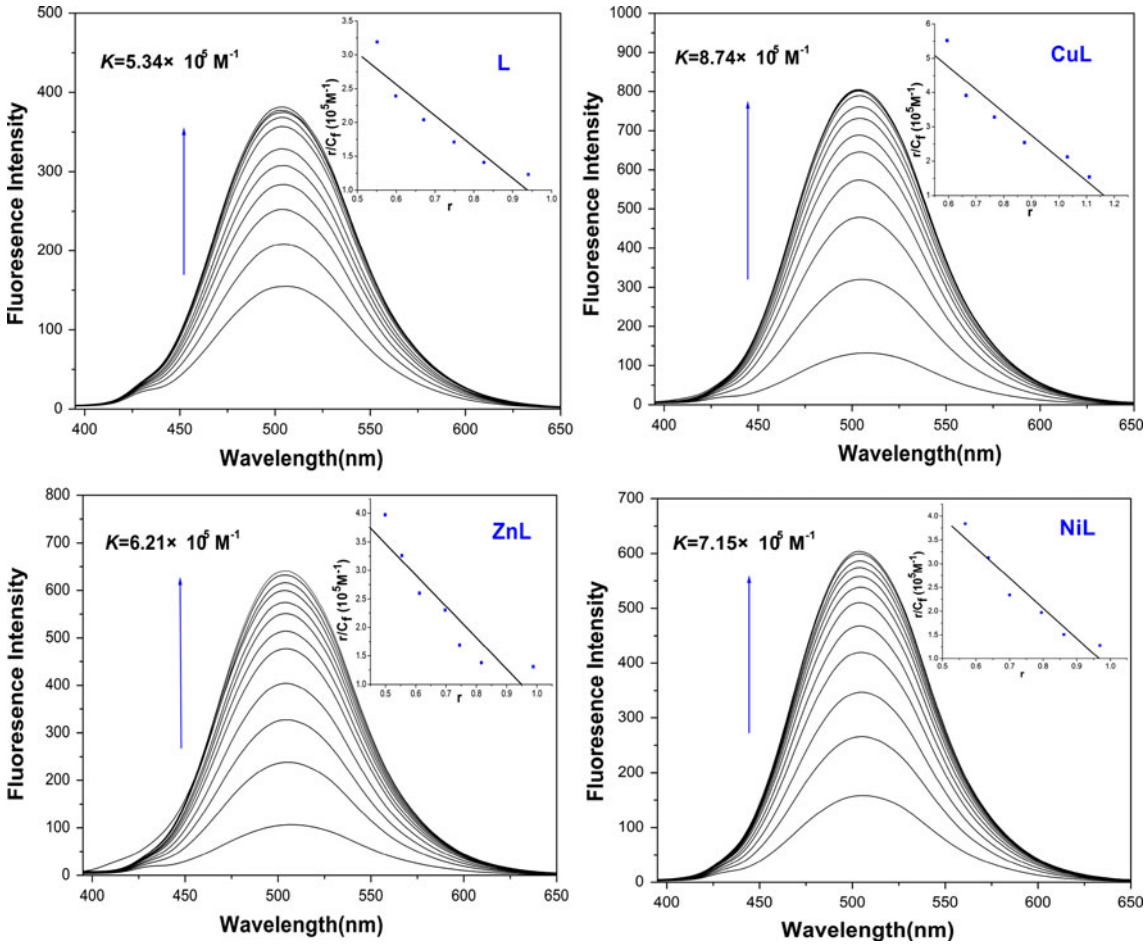

Fig. 4 Emission enhancement spectra of compounds (10 μM) in the absence and presence of increasing amounts of CT-DNA (2.5, 5, 7.5, 10, 12.5, 15, 17.5, 20, 22.5, 25, 27.5, 30 μM; *Arrow* shows the emission intensity changes upon increasing CT-DNA concentration. *Inset*: Scatchard plot of the fluorescence titration data of compounds, $K_L = 5.34 \times 10^5\ M^{-1}$. $K_{CuL} = 8.74 \times 10^5\ M^{-1}$. $K_{ZnL} = 6.21 \times 10^5\ M^{-1}$. $K_{NiL} = 7.15 \times 10^5\ M^{-1}$

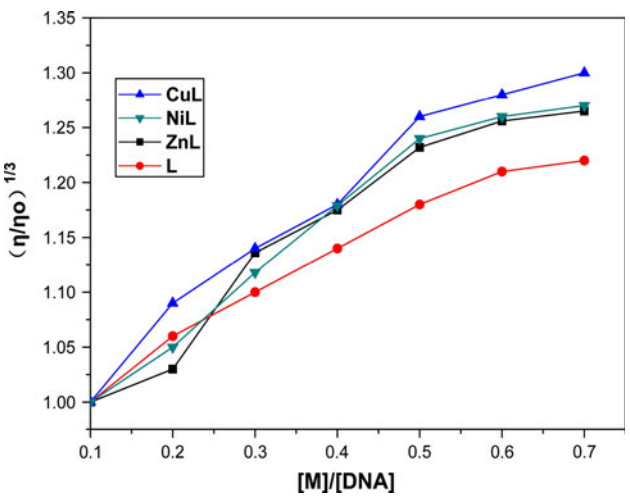

Fig. 5 Effect of increasing amounts of L, CuL, ZnL and NiL on the relative viscosity of CT-DNA at 25.0 ± 0.1 °C, [DNA] = 5.0 μM

$\times 10^5\ M^{-1}$ (ZnL) and $K_q = 1.06 \times 10^5\ M^{-1}$ (NiL). The quenching plots illustrate that the quenching of EB bound to DNA by these compounds is in good agreement with the linear Stern–Volmer equation and the binding ability follows the order CuL > NiL > ZnL > L, in agreement with the fluorescence and viscosity measurements. Furthermore, the quenching constants suggest that the quenching mode is static rather than dynamic, and the interaction of all the compounds with DNA should be by intercalation [42].

Antioxidant activity

Figure 7 depicts the inhibitory effect of the compounds on $OH^{\bullet}$ radicals. The inhibitory activity of the compounds is marked, and the suppression ratio increases with increasing concentration of the test compound. The sequence of the suppression ratio is CuL > NiL > ZnL > L. We compared the present compounds with the well-known natural

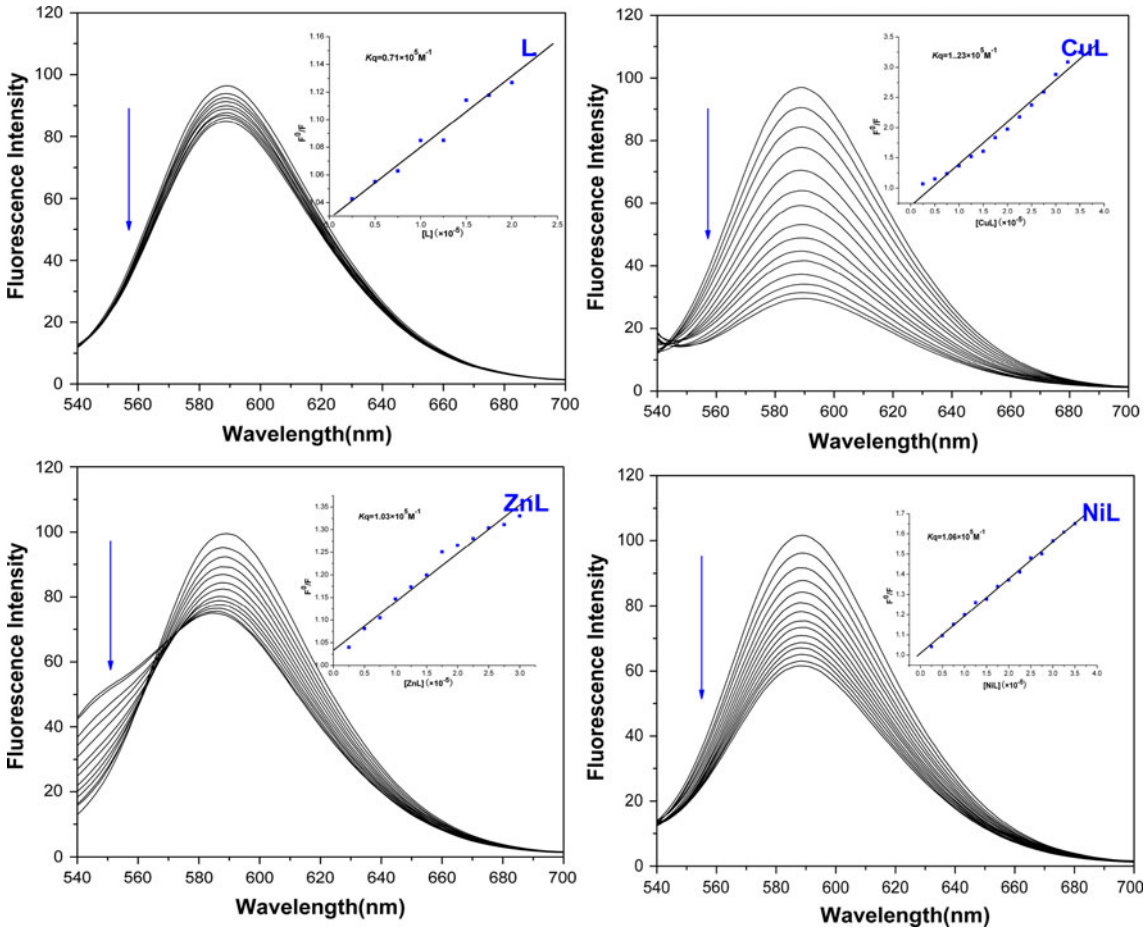

Fig. 6 Emission spectra of DNA-EB system (10 μM DNA and 0.33 μM EB), $\lambda_{ex} = 521$ nm, $\lambda_{em} = 540$–700 nm, in the presence of (0, 2.5, 5, 7.5, 10, 12.5, 15, 17.5, 20, 22.5, 25, 27.5 and 30 μM) ligand, CuL, ZnL and NiL. *Arrow* shows the emission intensity changes upon increasing compound concentration. *Inset*: Stern–Volmer plot of the fluorescence titration of compounds

antioxidants mannitol and vitamin C, using the same method as reported in a previous paper [43]. The 50% inhibitory concentration (IC_{50}) value of mannitol is about 9.6 mM. According to the antioxidant experiments, the IC_{50} of CuL is 3.08 μM, which implies that CuL exhibits better scavenging activity than L, ZnL and NiL, as well as mannitol and vitamin C. We suggest that the mechanism of action of CuL involves the redox process of Cu(II) [44, 45].

Solid-state fluorescence spectra

The fluorescence from the free ligand CuL and NiL is weak; however, the Zn(II) complex exhibits light Kelly fluorescence ($\lambda_{em} = 513$ nm). The solid-state fluorescence emission is readily observed with the naked eye under UV light, as shown in Fig. 8. The Zn(II) complex is the first example of a light Kelly fluorescence complex with 2-oxo-quinoline-3-carbaldehyde-4- aminophenazone Schiff base.

As observed, the coordination of Zn(II) clearly changes the emission efficiency of the ligand, which can be attributed to the increase in the ligand's conformational rigidity, thus favouring a more planar and conjugated structure [46].

Conclusion

In this work, a new 2-oxo-quinoline-3-carbaldehyde Schiff base ligand and its Cu(II), Zn(II) and Ni(II) complexes have been synthesized and characterized. The binding modes of these compounds with CT-DNA have been studied. The photophysical and viscosity measurements indicate that the compounds interact with CT-DNA through intercalative binding modes. In addition, the metal complexes show higher affinities than the free ligand, which can be attributed to the more planar structure owing to upon coordination to the metal. The antioxidant activities of the compounds were also investigated. CuL exhibits the most effective scavenging of hydroxyl radical among these compounds. Finally, the solid-state fluorescence

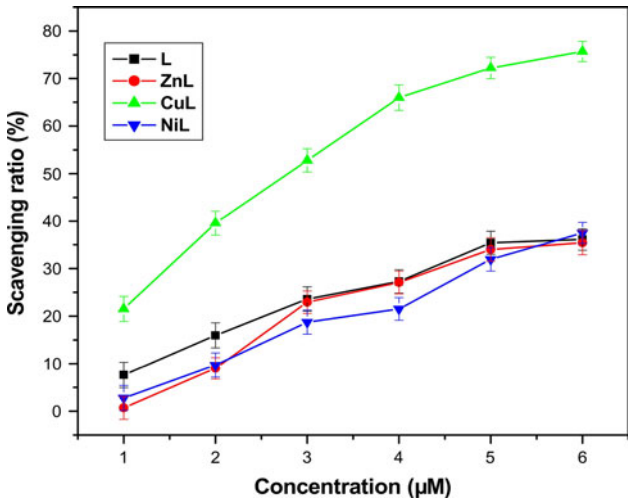

Fig. 7 Scavenging effect of compounds on hydroxyl radicals. Experiments were performed in triplicate. Values are expressed as mean ± standard deviation ($n = 1$). IC_{50} (L) = 7.95 μM, IC_{50} (NiL) = 7.47 μM, IC_{50} (CuL) = 3.08 μM, IC_{50} (ZnL) = 7.85 μM

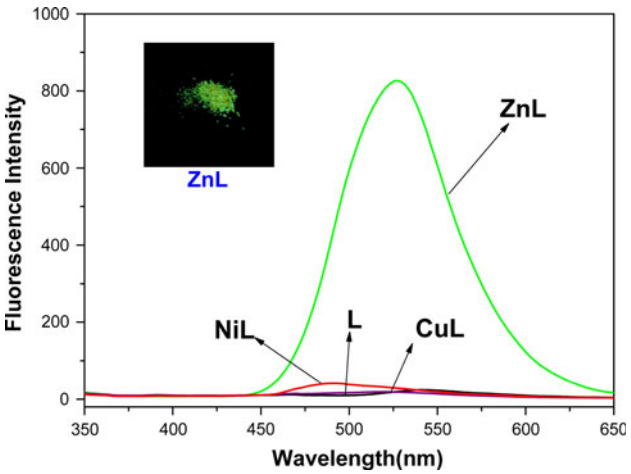

Fig. 8 Solid-state fluorescence spectrum of compounds (L, CuL, ZnL, NiL) and fluorescence image of ZnL under UV light, Slit (excite and emit) = 1.5 nm. $\lambda_{ex} = 393$ nm, $\lambda_{em} = 513$ nm

experiments suggest potential application as a new class of efficient Kelly emitter.

Supplementary data

Crystallographic data for the structural analysis have been deposited with the Cambridge Crystallographic Data Centre, CCDC (795295, 796448). Copy of this information may be obtained free of charge from the Director, CCDC, 12 Union Road, Cambridge, CB2 1EZ, UK (fax: +44-1223-336033; e-mail: deposit@ccdc.cam.ac.uk or http://www.ccdc.cam.ac.uk/deposit).

Acknowledgments This work is supported by the National Natural Science Foundation of China (20975046).

References

1. Leininger S, Olenyuk B, Stang PJ (2000) Chem Rev 100:853–907
2. Erkkila KE, Odem DT, Barton JK (1999) Chem Rev 99: 2777–2796
3. Tarushi AT, Raptopoulou CP, Psycharis V, Terzis A, Psomas G, Kessissoglou DP (2010) Bioorg Med Chem 18:2678–2685
4. Liu YJ, Zeng CH, Huang HL, He LX, Wu FH (2010) Eur J Med Chem 45:564–571
5. Liu ZC, Wang BD, Yang ZY, Li Y, Qin DD, Li TR (2009) Eur J Med Chem 44:4477–4484
6. Wang BD, Yang ZY, Lü MH, Hai J, Wang Q, Chen ZN (2009) J Org-Met Chem 25:4069–4075
7. Barron GA, Bermano G, Gordon A, Kong Thoo Lin P (2010) Eur J Med Chem 45:1430–1437
8. Mukherjee S, Basu C, Chowdhury S, Chattopadhyay AP, Ghorai A, Ghosh U, Stoeckli-Evans H (2010) Inorg Chim Acta 36: 32752–32761
9. Duh P-D, Wu S-C, Chang L-W, Chu H-L, Yen W-J, Wang B-S (2009) Food Chem 114:87–92
10. Andaloussi M, Moreau E, Masurier N, Lacroix J, Gaudreault RC, Chezal JM, Laghdach AE, Canitrot D, Debiton E, Teulade JC, Chavignon O (2008) Eur J Med Chem 43:2505–2517
11. Chellan P, Nasser S, Vivas L, Chibale K, Smith GS (2010) J Org-Met Chem 695:2225–2232
12. Khanye SD, Smith GS, Lategan C, Smith PJ, Gut J, Chibale K, Rosenthal PJ (2010) J Inorg Biochem 104:1079–1083
13. Padhye S, Kauffman GB (1985) Coord Chem Rev 63:127–160
14. Wang L, Zhu Y, Yang Z, Wu J, Wang Q (1991) Polyhedron 10:2477–2481
15. Anna AA, Jordi BB, Stephen N, Ramón V (2008) Inorg Chem 47:11910–11919
16. Julie ER, Anna AA, Stephen N, Ramón V (2006) J Am Chem Soc 128:5992–5993
17. Wang P, Leung CH, Ma DL, Yan SC, Che CM (2010) Chem Eur J 16:6900–6911
18. Marta MB, Sander JW, Robert MH, Daniele A, Eduardo CEA, Jordi BB, Arjan WK (2010) Dalton Trans 39:4541–4550
19. Daniele A, Eduardo C, Escudero A, Jordi BB, Arjan WK (2010) Dalton Trans 39:8733–8740
20. Bukhari SB, Memon S, Mahroof-Tahir M, Bhanger MI (2009) Spectrochim Acta A Mol Biomol Spectrosc 71:1901–1906
21. Afanas'ev IB, Ostrakhovitch EA, Mikhal'lchi EV, Ibragimova GA, Korkina LG (2001) Biochem Pharma 61:677–684
22. Botelho FV, Alvarez-Leite JI, Lemos VS, Pimenta AMC, Calado HDR, Matencio T, Miranda CT, Pereira-Maia EC (2007) J Inorg Biochem 101:935–943
23. Wang Q, Yang ZY, Qi GF, Qin DD (2009) Eur J Med Chem 44:2425–2433
24. Ihara Y, Chuda M, Kuroda S, Hayabara T (1999) J Neurol Sci 170:90–95
25. Singh MK, Chandra A, Singh B, Singh RM (2007) Tetra Lett 48:5987–5990
26. Liu ZC, Wang BD, Yang ZY, Li TR, Li Y (2010) Inorg Chem Comm 13:606–608
27. Czarny A, Boykin DW, Wood AA, Nunn CM, Neidle S, Zhao M, Wilson WD (1995) J Am Chem Soc 117:4716–4717
28. Winterbourn CC (1981) Biochem J 198:125–131
29. Winterbourn CC (1979) Biochem J 182:625–628
30. Guo ZY, Xing RE, Liu S, Yu HH, Wang PB, Li CP, Li PC (2005) Bioorg Med Chem Lett 15:4600–4603

31. Marklund SL, Adolfsson R, Gottfries CG, Winblad B (1985) J Neurol Sci 67:319–325
32. Pyle MA, Rehmann PJ, Meshoyrer R, Kumar JN, Turro JN, Barton KJ (1989) J Am Chem Soc 111:3053–3063
33. Kumar CV, Asuncion HE (1993) J Am Chem Soc 115:8547–8553
34. Xu H, Yi L, Zhang P, Du F, Zhou BR, Wu J, Liu JH, Liu ZG, Ji LN (2005) J Biol Inorg Chem 10:529–538
35. Friedman AE, Chambron JC, Sauvage JP, Turro NJ, Barton JK (1990) J Am Chem Soc 112:4960–4962
36. Wang BD, Yang ZY, Li TR (2006) Bioorg Med Chem 14:6012–6021
37. Yang ZY, Wang Y, Wang Y (2007) Bioorg Med Chem Lett 17:2096–2101
38. Izumrudov VA, Zhiryakova MV, Goulko AA (2002) Langmuir 18:10348–10356
39. Liu J, Zhang T, Lu T, Qu L, Zhou H, Zhang Q, Ji L (2002) J Inorg Biochem 91:269–276
40. Tarushi A, Psomas G, Raptopoulou CP, Kessissoglou DP (2009) J Inorg Biochem 103:898–905
41. Howe GM, Wu KC, Bauer WR (1976) Biochem 19:339–347
42. Wang BD, Yang ZY, Wang Q, Cai TK, Crewdson P (2006) Bioorg Med Chem 14:1880–1888
43. Li TR, Yang ZY, Wang BD, Qin DD (2008) Eur J Med Chem 43:1688–1695
44. Schepetkin I, Potapov A, Khlebnikov A, Korotkova E, Lukina A, Malovichko G, Kirpotina L, Quinn MT (2006) J Biol Inorg Chem 11:499–513
45. Patel MN, Gandhi DS, Parmar PA (2010) Inorg Chem Comm 13:618–621
46. Nijegorodov NI, Downey WS (1994) J Phys Chem 98:5639–5643